The following article appeared in Advanced Materials Letters 8(7): 768-772 (2017); and may be found at: http://dx.doi.org/10.5185/amlett.2017.1452

Magnetic, Thermal, and Magnetocaloric Properties of $Ni_{50}Mn_{35}In_{14.5}B_{0.5}$ Ribbons

Sudip Pandey [1*], Abdiel Quetz[1], P. J. Ibarra-Gaytan[2], C. F. Sanchez-Valdes[3], Anil Aryal[1], Igor Dubenko[1], Dipanjan Mazumdar[1], J.L. Sanchez Llamazares[2,*], Shane Stadler[4], and Naushad Ali[1]

[1]*Department of Physics, Southern Illinois University, Carbondale, IL 62901 USA*
[2]*Instituto Potosino de Investigación Cientıfica y Tecnológica A.C., Camino a la Presa San Jose 2055, Col. Lomas 4[a] sección, San Luis Potosı, S.L.P. 78216, Mexico*
[3]*División Multidisciplinaria, Ciudad Universitaria, Universidad Autónoma de Ciudad Juárez (UACJ), calle José de Jesús Macías Delgado # 18100, Ciudad Juárez 32579, Chihuahua, México*
[4]*Department of Physics & Astronomy, Louisiana State University, Baton Rouge, LA 70803 USA*

*Corresponding author: E-mail: sudip@siu.edu (Sudip Pandey) and jose.sanchez@ipicyt.edu.mx (J.L. Sánchez Llamazares)

Abstract

The structural, thermal, magnetic, and magnetocaloric properties of $Ni_{50}Mn_{35}In_{14.5}B_{0.5}$ melt-spun ribbons have been investigated using room-temperature x-ray diffraction (XRD), differential scanning calorimetry (DSC), and magnetization measurements. Magnetic and structural transitions were found to coincide in temperature leading to large magnetocaloric effects associated with the first-order magnetostructural phase transition. In comparison to the bulk $Ni_{50}Mn_{35}In_{14.5}B_{0.5}$ alloys, both the martensitic transition temperature (T_M) and Curie temperature (T_C) shifted to lower temperatures. The MCE parameters were found to be comparable to those reported for bulk $Ni_{50}Mn_{35}In_{14.5}B_{0.5}$ Heusler alloys and $Ni_{48}Mn_{39}In_{13-x}B_x$ ribbons. A comparison of magnetic properties and magnetocaloric effects in $Ni_{50}Mn_{35}In_{14.5}B_{0.5}$ alloys as a ribbons and in their bulk form has been shown in detail. The roles of the magnetic and structural changes on the transition the temperatures of the ribbons are discussed.

Keywords: 'Heusler alloys', 'Martensitic transition', 'Ribbons', and 'Magnetocaloric effects'

Introduction

Magnetic materials that exhibit large magnetocaloric effects (MCE), i.e., the ability to absorb or release heat when exposed to a magnetic field, are of interest for refrigeration devices **[1]**. In comparison to compressor-based systems, magnetic refrigeration based on MCE eliminates toxic gas emission, is a relatively quiet technology, i.e., no compressors, and has a higher energy efficiency based on theoretical Carnot efficiency. The simultaneous change in the structure and the magnetic properties induced by the magnetic field is often accompanied by a large MCE **[2]**. The Ni-Mn-In Heusler systems exhibit a tunable magnetostructural phase transition around room temperature with large MCE values **[3]**, and other magneto-responsive phenomena (magnetoresistance **[4]**, magnetostriction **[5]**, etc.). Additionally, for Ni-Mn-In systems, it's relatively low cost of raw materials, low energy cost during fabrication etc. make it advantageous for applications.

Until now, the Ni-Mn-In based Heusler alloys have been produced as bulk materials by means of conventional melting techniques followed by lengthy thermal annealing **[6-8]**. Recently, much research is being carried out to develop new magnetocaloric materials in the form of ribbons **[9-14]**. The advantage of using ribbons as a raw materials, can be further consolidated into thicker plates by strip casting or sintering in magnetic refrigerators which improve the technical characteristics of refrigeration unit by optimizing the heat transfer between the heat-exchange liquid and working body **[15]**. Previous studies indicate that ribbons obtained by the melt-spinning method significantly decrease the grain size as a result of fast cooling, causing a reduction of annealing time, and the ribbons exhibits very small magnetic hysteresis **[16]**. A more recently reported

melt-spinning technique effectively promotes more homogeneous materials, shortened annealing stage, and improved MCE properties **[17]**. It has recently been observed that the effect of substitution of In by B in annealed Ni-Mn-In Heusler alloy ribbons strongly affects the magnetic state of the martensitic phase, the magnetic entropy change, and the exchange bias properties of the ribbons **[18]**.

In previous work, we report the magnetic, transport and magnetocaloric properties of B doped bulk Ni-Mn-In Heusler alloys **[19]**. In view of the current interest and great potential of these compounds as magnetocaloric materials near room temperature, here we report the synthesis and properties of the $Ni_{50}Mn_{35}In_{14.5}B_{0.5}$ by rapid solidification using the melt-spinning technique. We carried out a detailed study of the crystal structure, magnetic states, martensitic phase transition temperature, magnetic entropy changes, and refrigeration capacity (RC) of the $Ni_{50}Mn_{35}In_{14.5}B_{0.5}$ as-solidified melt-spun ribbons.

Experimental techniques

Polycrystalline ingots of $Ni_{50}Mn_{35}In_{14.5}B_{0.5}$ were prepared by arc-melting in a high-purity argon atmosphere. The ingots were re-melted four times and subsequently annealed at 850 °C for 48 hours under vacuum, and then slowly cooled to room temperature. From the samples obtained by arc-melting, rapidly solidified ribbons (with thicknesses ≈ 30–35 μm) were produced by the Edmund Buhler model SC melt spinner system in an argon atmosphere at a wheel linear speed of 20 m/s. The crystal structure of the sample was studied using a high resolution Rigaku Smartlab diffractometer employing Cu-Kα radiation. The pattern was measured on a powdered sample. The thermal behavior was studied using a differential scanning calorimetry (DSC) by employing a TA Instruments model Q200 DSC (with a sweep rate of 10 K/min during heating and cooling) in the temperature range of 200-400K. The magnetic properties were measured at temperatures ranging from 5 to 400 K and in magnetic fields μ_oH up to 5 T in a Quantum Design 9 T- PPMS, using the vibrating sample magnetometry. The magnetic field was applied along the major length of the ribbon samples (typically, ~4 mm long) to minimize the demagnetizing field effect. The ΔS_M was estimated from the isothermal magnetization curves near the martensitic/magnetic transition temperature using the Maxwell relation [20].The refrigerant capacity, *RC,* was estimated from the $\Delta S_M(T)$ curves.

Results and discussion

The room temperature X-ray diffraction (XRD) pattern of a $Ni_{50}Mn_{35}In_{14.5}B_{0.5}$ ribbons is shown in **Figure 1**. A mixture of austenitic (high temperature) and martensitic (low temperature) phases was observed and the martensitic phases were found to be in the tetragonal state. As seen from **Figure 1**, the low temperature martensitic phase dominates and only traces of the high temperature austenitic phase were present at room temperature. The XRD pattern of $Ni_{50}Mn_{35}In_{14.5}B_{0.5}$ ribbons are similar to those of the Ni-Mn-In based Heusler alloys in the phase coexistence region exhibiting a MST near room temperature **[19]**.

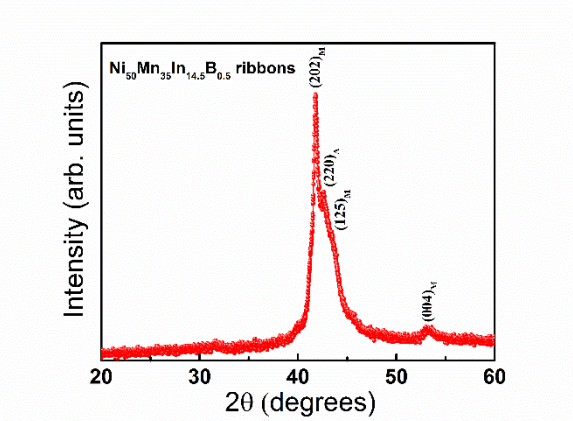

Figure 1. Room temperature X-ray powder diffraction obtained for a $Ni_{50}Mn_{35}In_{14.5}B_{0.5}$ melt-spun ribbons.

The temperature dependence of the magnetization (M) of the $Ni_{50}Mn_{35}In_{14.5}B_{0.5}$ as-solidified melt-spun ribbon in the presence of 5 mT ~~50 Oe~~ magnetic field is shown in **Figure 2(a)**. The measurements have been first carried out during heating after the samples were cooled from 400 K to the lowest temperature (5 K) at zero magnetic field (i.e, in the zero-field-cooled (ZFC) mode), and subsequently in field-cooled and field-heated regimes ~~measurements~~. ~~In case of field cooling (FC) measurements, the sample was cooled to 5 K in the presence of a 100 Oe magnetic field.~~ A second order transition was observed from a paramagnetic austenitic (PA) to a ferromagnetic austenitic (FA) phase at T_C = 300 K, and a first order magnetostructural transition (MST) was observed from a ferromagnetic austenitic (FA) to low magnetization martensitic phase at T_M = 260 K. The high field (μ_oH = 5 T) M(T) data are shown in the inset of **Figure 2(a)**. The maximum difference in magnetization, ΔM, at T_M was found to be ≈ 50 Am^2kg^{-1} for the ribbons at T = 280 K ~~at~~ and μ_oH = 5 T. The presence of thermal hysteresis and the jump-like change in magnetization at T_M are typical for first order structural (martensitic) transitions.

The sample shows a splitting of the ZFC and FC magnetization curves at low temperature (T < 110 K) (**see Figure 2(a)**). The splitting of the low field ZFC and FC curves at temperatures lower than T_{CM} is typical for the bulk Heusler alloys, where exchange bias (EB) phenomena are observed owing to the coexistence of antiferromagnetic and ferromagnetic interactions between Mn atoms in the martensite structure **[14]**.

(a)

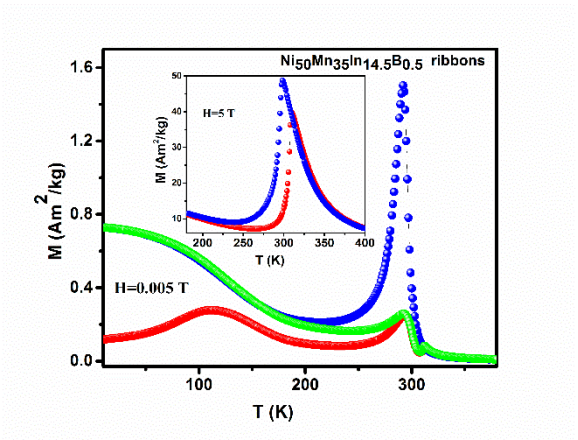

(b)

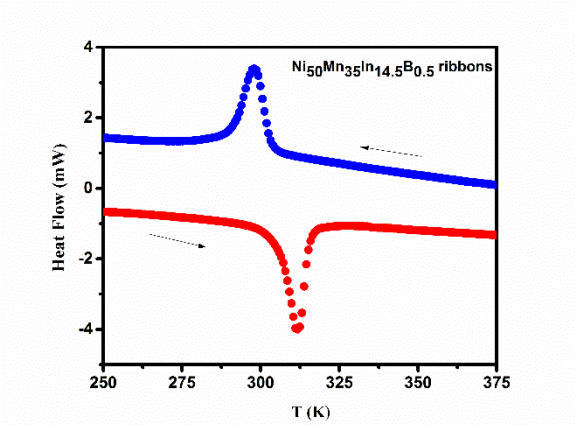

Figure 2. (a) Temperature dependence of the magnetization measured under static magnetic fields of ~~0.005~~ 5 mT and 5 T (inset) for the $Ni_{50}Mn_{35}In_{14.5}B_{0.5}$ ribbons. **(b)** DSC scans for $Ni_{50}Mn_{35}In_{14.5}B_{0.5}$ as-solidified melt-spun ribbons. **SUDIP, In (a), please, indicate the ZFC, FC and FC pathways of the M(T) curves**

In comparison to the bulk $Ni_{50}Mn_{35}In_{14.5}B_{0.5}$ alloys, both the martensitic transition temperature (T_M) and Curie temperature (T_C) shifted to lower temperatures **[19]**. A shift of the MST from 300 K to 260 K, as determined from the maximum change of the temperature dependent dM/dT in the magnetization heating curve has been observed. The fabrication of these alloys by rapid solidification leads to a reduction in the average grain size which lead to the decrease in the structural transition temperature **[21, 22]**. The first order nature of the phase transitions in $Ni_{50}Mn_{35}In_{14.5}B_{0.5}$ as-solidified melt-spun ribbons has been confirmed by the temperature hysteresis of the heat flow transition peaks obtained from DSC measurements (**Figure 2(b)**). The large endothermic/exothermic peaks, observed during heating/cooling cycles, are related to the latent heat of the first-order magnetostructural transition from the low magnetization martensitic state to the ferromagnetic state. The temperature hysteresis of the heat flow (ΔT_{hyst}) of about 10 K between heating and cooling cycles detected from DSC measurements are consistent with the data obtained from the bulk Heusler alloys.

(a)

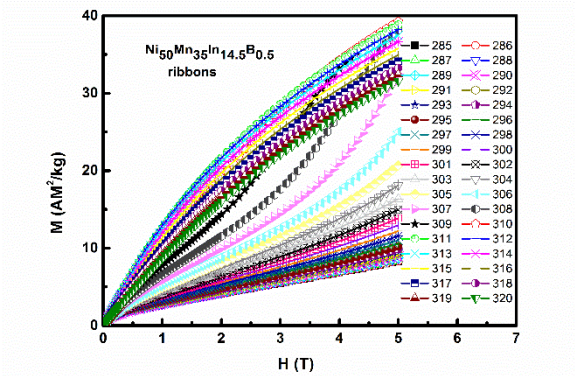

(b)

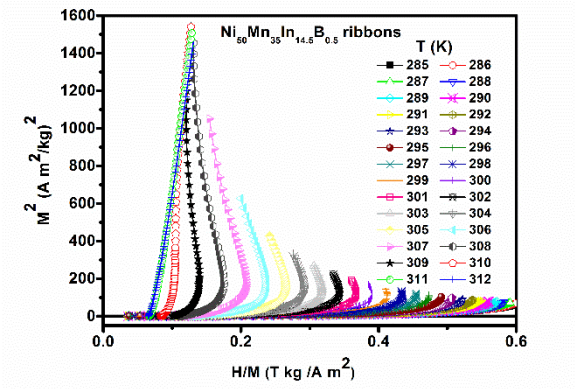

Figure 3. (a) Isothermal magnetization curves measured up to a maximum magnetic field of 5 T, and (b) the corresponding Arrott plots for a $Ni_{50}Mn_{35}In_{14.5}B_{0.5}$ melt-spun ribbons. **SUDIP, Please, the HORIZONTAL AXIS, should be** $\mu_o H/M$

Isothermal magnetization curves M(μ_oH) for $Ni_{50}Mn_{35}In_{14.5}B_{0.5}$ ribbons in the vicinity of the FOT and SOT are shown in **Figure 3(a)**. The magnetization isotherms were found to show metamagnetic-like behavior in close vicinity to the martensitic transition temperature and are characteristic of ferromagnetic-paramagnetic transitions near the Curie temperature**.** In order to determine the type and order of the magnetic transitions, Arrott plots of M^2 as a function of μ_oH/M were plotted in the temperature interval, ΔT = 1 K. **Figure 3(b)** shows the Arrott plots of $Ni_{50}Mn_{35}In_{14.5}B_{0.5}$ ribbons for $\mu_o H \leq 5$ T and 285 K ≤ T ≤ 312 K, from which the Curie temperature was determined from the temperature at which the μ_oH/M vs M^2 curves change sign of curvature. The values obtained from the Arrott plots were comparable to those obtained from the maximum of the differential magnetization (dM/dT) of the M(T) curves.

Magnetic hysteresis causes thermal losses at the FOT. This hysteretic loss is due to a field induced first order martensitic transition **[23]**. This loss reduces the RC, and is therefore an unwanted characteristic in a magnetic refrigerant system. The estimated loss was calculated from the difference in area under the hysteresis curves of M(μ_oH). For clarity, typical M(μ_oH) curves for both magnetizing and demagnetizing fields up to 2 T for $Ni_{50}Mn_{35}In_{14.5}B_{0.5}$ ribbons are shown in Figure 4. The hysteresis loss (HL) was estimated from the enclosed area between the magnetizing and demagnetizing M(μ_oH) curves and plotted in the inset of Figure 4. The maximum HL across the MST for a magnetic change of 2 T was found to be 2.5 J/kg, which is significantly lower than that observed in the bulk Heusler system **[24]**.

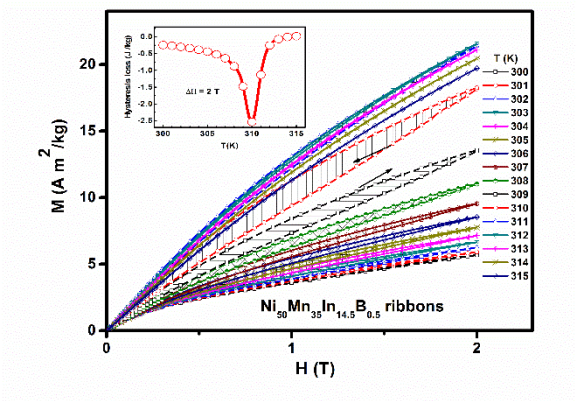

Figure 4. Field-up and field-down isothermal magnetization curves for a $Ni_{50}Mn_{35}In_{14.5}B_{0.5}$ as-solidified melt-spun ribbons up to H=2 T. The inset shows the hysteresis loss (HL) as a function of temperature across the MST for a magnetic field change of 2 T. **SUDIP, (a) The HORIZONTAL AXIS, should be ; (b) Larger letters and number are needed at the inset.**

The magnetic entropy changes (ΔS_M) in the vicinity of the MST and SOT for different magnetic fields (ΔH) were calculated using the Maxwell relation, $(\partial S/\partial H)_T = (\partial M/\partial T)_H$, from the magnetization isotherms (see **Figure 4**) measured at different temperatures. As shown in Figure 5(a) MCE has been observed in the vicinity of T_M and T_C for $Ni_{50}Mn_{35}In_{14.5}B_{0.5}$ ribbons. The peak values of the magnetic entropy change $|\Delta S_M^{peak}|$ in the vicinity of T_M and T_C for $\mu_o\Delta H = 5T$ were found to be 17 J/kg K and 5 J/kg K, respectively. This large value is due to the jump-like change of magnetization (refer to **Figure 2(a)**) corresponding to the first-order magnetostructural transition. The MCE parameters were found to be comparable to those

(a)

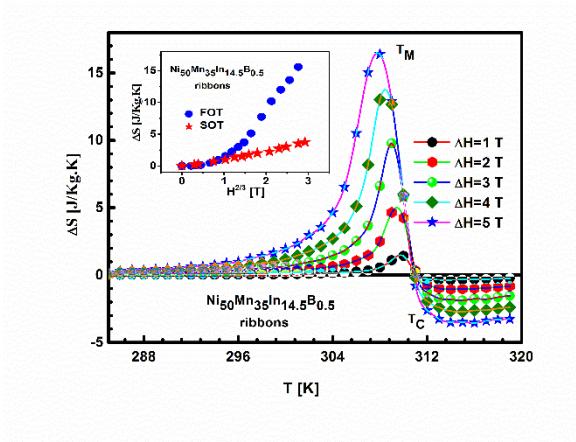

(b)

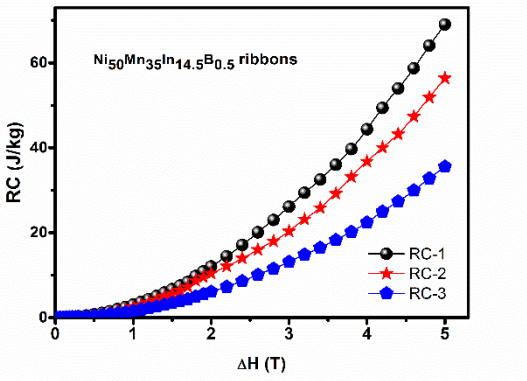

Figure 5: (a) The magnetic entropy change (ΔS_M) of a $Ni_{50}Mn_{35}In_{14.5}B_{0.5}$ ribbons with the temperature in the vicinity of the FOT and SOT. The inset shows the maximum entropy change $|\Delta S^{peak}|$ as a power function of magnetic field change $[\mu_o\Delta H)^{2/3}]$ collected at temperature (T) in the vicinity of the FOT and SOT. (b)The refrigerant capacities, *RC*-1, *RC*-2, and *RC*-3 as a function of change in magnetic field change for a $Ni_{50}Mn_{35}In_{14.5}B_{0.5}$ as-solidified melt-spun ribbons at FOT. **SUDIP: (A) In figure (b) the**

HORIZONTAL AXIS, should be $\mu_o\Delta H$; (B) In the inset of figure (a) the horizontal axis should be $(\mu_o\Delta H)^{2/3}$, while the vertical $|\Delta S^{max}|$; (c) In figure (a) multiply μ_o by the ΔH values. Larger letters and number are needed at the inset of figure (a).

observed for bulk $Ni_{50}Mn_{35}In_{14.5}B_{0.5}$ Heusler alloys and $Ni_{48}Mn_{39}In_{13-x}B_x$ ribbons **[18, 19]**. For magnetic refrigeration materials with second order phase transition, the mean field theory predicts that the value of isothermal magnetic entropy change ΔS_M near the SOT is related to the field according to the relation **[25]**,

$$|\Delta S_M^{peak}| \propto H^{2/3} (\mu_o\Delta H)^{2/3}$$

$|\Delta S_M^{peak}|$ was plotted as a power function of magnetic field, $H^{2/3}$, collected at a given temperature (T) in the vicinity of FOT and SOT in inset of **Figure 5(a)**. The linear fit to the data in the inset of **Figure 5(a)** clearly shows that the above relationship is valid for $Ni_{50}Mn_{35}In_{14.5}B_{0.5}$ ribbons near T_C, whereas the FOT do not obey the $(\mu_o\Delta H)^{2/3}$ $H^{2/3}$ law due to the discontinuous transition. Hence, the studied ribbons at T_C are governed by long-range interactions, and the magnetic transition FM to PM belongs to the second order magnetic phase transitions. Our result is consistent with theoretical result.

Another important parameter to evaluate the potential of the MCE of a given material is the ideal refrigeration capacity (RC). *RC,* was estimated from the $\Delta S_M(T)$ curves at T_M (a) by calculating the product $|\Delta S_M^{peak}| \times \delta T_{FWHM}$ (referred to as *RC*-1), where $\delta T_{FWHM} = T_{hot} - T_{cold}$, corresponds to the full-width at half-maximum of the $\Delta S_M(T)$ curves; (b) by integrating the curve over the FWHM using $RC=\int_{T_{cold}}^{T_{hot}} \Delta S_M(T)dT$ (*RC*-2), and (c) by maximizing the product $\Delta S_M \times \delta T$ below the $\Delta S_M(T)$ curve (*RC*-3; Wood and Potter criterion). The refrigerant capacities, *RC*-1, *RC*-2, and *RC*-3 as a function of the magnetic field change for $Ni_{50}Mn_{35}In_{14.5}B_{0.5}$ as-solidified melt-spun ribbons are shown in **Figure 5(b)**. The refrigeration capacity (RC) in the vicinity of T_M was found to be 70 J/kg for a magnetizing field of 5 T. These values of RC are comparable to those of bulk $Ni_{50}Mn_{35}In_{14.5}B_{0.5}$ systems near room temperature **[19]**.

Conclusion

In summary, we have reported the magnetic properties and magnetocaloric effects in $Ni_{50}Mn_{35}In_{14.5}B_{0.5}$ melt-spun Heusler alloy ribbons, with small mass and thickness. Magnetic and structural transitions were found to coincide in temperature leading to large magnetocaloric effects associated with the first-order magnetostructural phase transition. The MCE parameters were found to be comparable to those observed in bulk $Ni_{50}Mn_{35}In_{14.5}B_{0.5}$ Heusler alloys and $Ni_{48}Mn_{39}In_{13-x}B_x$ ribbons. These characteristics suggest that $Ni_{50}Mn_{35}In_{14.5}B_{0.5}$ melt-spun Heusler alloys ribbons are promising materials for ongoing research on magnetocaloric effects and related properties.

Acknowledgements

This work was supported by the Office of Basic Energy Sciences, Material Science Division of the U.S. Department of Energy, DOE Grant No. DE-FG02-06ER46291 (SIU) and DE-FG02-13ER46946 (LSU). The authors acknowledge financial support received from Laboratorio Nacional de Investigaciones en Nanociencias y Nanotecnología (LINAN, IPICyT) and CONACyT, Mexico under grants CB-2012-01-183770 and CB-2012-01-176705.

Author's contributions

Naushad, Shane, Dipanjan, Igor, J.L. Sanchez Llamazares, and Sudip gather the ideas and make a plan to do the experiments. Sudip, Abdiel, P. J. Ibarra, J.L. Sanchez Llamazares and C.F. Sanchez-Valdés performed the experiments. Data analysis is done by Sudip, Anil, P. J. Ibarra, and C. F. Sanchez. Sudip and P. J. Ibarra wrote the paper. Authors have no competing financial interests.

References

(a) Scientific article

1. Franco, V.; Blazquez, S. J.; Ingale, B.; Conde, A.; Annu. Rev. Mater. Res., 2012, 42, 305-342.
DOI: 10.1146/annurev-matsci-062910-100356
2. Pecharsky, A.; Gschneidner, K.; Pecharsky, V.; *J. Phys. Rev. Lett.,* **1997,** 78 4494.
DOI: 10.1103/PhysRevLett.78.4494
3. Krenke, T.; Duman, E.; Acet, M.; Wassermann, E.; Moya, X.; Ma~nosa, L.; Planes, A.; *Nat. Mater.,* **2005**, 4, 450.
DOI: 10.1038/415150a 10.1038/nmat1395
4. Provenzano, V.; Shapiro, J. A.; Shull, D. R.; *Nature (London)*, **2004,** 429, 853.
DOI: 10.1038/nature02659
5. Serrate, D.; Teresa, J. M.; Cordoba, R.; Yusuf, M. S.; Solid State Comm., **2007**, 142, 363-367.
DOI: 10.1016/j.ssc.2007.02.042
6. Pathak, A.; Khan, M.; Dubenko, I.; Stadler, S.; Ali, N.; *Appl. Phys. Lett.*, **2007**, 90, 262504.
DOI: 10.1063/1.2752720
7. Dubenko, I.; Quetz, A.; Pandey, S.; Aryal, A.; Rodionov, I; Prudnikov, V.; Lahderanta, E.; Samanta, T.; Saleheen, A.; Stadler, S.; Ali, N.; J. *Magn. Magn. Mater.*, **2015**, 383,186–189.
DOI: 10.1016/j.jmmm.2015.11.025
8. Khan, M.; Dubenko, I.; Stadler, S.; Ali, N.; *J. Appl. Phys.*, **2007**, 102, 113914.

DOI: 10.1063/1.2818016
9. Aliev, A.; Batdalov, A.; Kamilov, I.; Koledov, V.; Shavrov, V.; García, J.; Prida, V.; Hernando, B.; *App. Phys. Lett.,* **2010**, 97, 212505.
DOI: 10.1063/1.3521261
10. R. Caballero-Flores, T. Sánchez, W. O. Rosa, J. Garcíaa, L. González-Legarretaa, D. Serantesa, V. M. Pridaa, L. Escodac, J. J. Suñolc, B. Hernandoa, *J. Alloys and Compounds*, **2012**, 545, 216-221.
DOI: 10.1016/j.jallcom.2012.07.151
11. Sánchez Llamazares, J.; Sanchez, T.; Santos, J.; Perez, M.; Sanchez, M.; Hernando, B.; Escoda, L.; Suñol, J.; Varga, R.; *Appl. Phys. Lett*., **2008**, 92, 012513.
DOI: 10.1063/1.2827179
12. Hernando, B.; Sánchez Llamazares, J.; Santos, J.; Prida, V.; Baldomir, D.; Serantes, D.; Varga, R.; Gonzalez, J.; *Appl. Phys. Lett*., **2008**, 92, 132507.
DOI: 10.1063/1.2906361
13. Sánchez Llamazares, J.; García, C.; Hernando, B.; Prida, V.; Baldomir, D.; Serantes, D.; González, J.; *Appl. Phys. A*, **2011**, **103**, 1125.
DOI: 10.1007/s00339-010-6053-x
14. Sánchez Llamazares, J. L.; Flores-Zúñiga, H.; Sánchez-Valdés, C. F.; Ross, A. C.; García, C.; , *J. Appl. Phys.,* **2012**, 111, 07A932.
DOI: 10.1063/1.3676606
15. Theil Kuhn, L.; Pryds, N.; Bahl, C.; Smith, A.; *J. of Phys: Conf. Series*, **2011**, 303, 012082.
DOI: 10.1088/1742-6596/303/1/012082
16. Zhang, Y.; Zhang, L.; Zheng, Q.; Zheng, H.; Li, M.; Du, J.; Yan, A.; *Sci. Rep*., **2015**, 5, 11010.
DOI: 10.1038/srep11010 (2015)
17. Zheng, H.; Xia, M.; Liu, J.; Huang, Y.; Li, J.; *Acta. Mater,* **2011**, 59, 5692–5699.
DOI: 10.1016/j.actamat.2011.05.044
18. Zhao, G. X.; Hsieh, C. C.; Lai, J. H.; Cheng, X. J.; Chang, C. W.; Liu, W.; Zhang, D. Z.; *Scripta Materialia,* **2010**, 63, 250-253.
DOI: 10.1016/j.scriptamat.2010.03.067
19. Pandey, S.; Quetz, A.; Aryal, A.; Samanta, T.; Dubenko, I; Stadler, S.; Ali, N.; *J. Appl. Phys.*, **2015**, 117, 183905.
DOI: 10.1063/1.4921052
21. Kalbfleisch, A.; Matthews, G.; Jacques, J. P.; *Scripta Materialia*, **2016**, 114, 121.
DOI: 10.1016/j.scriptamat.2015.12.005
22. Quintana-Nedelcos, A.; Sánchez Llamazares, J.L.; Ríos-Jara, D.; Lara-Rodríguez, A. G.; García-Fernández, T.; *Phys. Stat. Sol. A*, **2013**,
210, 2159.
DOI: 10.1002/pssa.201329146
23. Khan, M.; Dubenko, I.; Stadler, S.; Ali, N.; *Appl. Phys. Lett.*, **2007**, 102, 113914.
DOI: 10.1063/1.2818016
24. Pathak, A.; Dubenko, I.; Mabon, J.; Stadler, S.; Ali, N.; *J. Phys. D: Appl. Phys*., **2008**, 41, 202004.
DOI: 10.1088/0022-3727/41/20/202004/meta
25. Oesterreicher H.; Parkar, F.; *J. of Appl. Phys*., **1984**, 55, 4334.
DOI: 10.1063/1.333046

(b) Book

20. Tishin, A.; Spichkin, Y.; The Magnetocaloric Effects and its Applications, IOP Publishing Ltd, **2003**.
DOI: 10.1201/9781420033373